

# Comparison of the $^{17}\text{O}$ NMR spectra of zeolites LTA and LSX

Jennifer E. Readman,<sup>a</sup> Clare P. Grey,<sup>a,\*</sup> Martine Ziliox,<sup>b</sup>  
Lucy M. Bull,<sup>c</sup> and Ago Samoson<sup>d</sup>

<sup>a</sup> Department of Chemistry, State University of New York at Stony Brook, Stony Brook, NY 11794-3400, USA

<sup>b</sup> Center for Molecular Medicine, State University of New York at Stony Brook, Stony Brook, NY 11794-5115, USA

<sup>c</sup> ChevronTexaco Energy Research and Technology Company, 100 Chevron Way, 10-2422, Richmond, CA 94802, USA

<sup>d</sup> National Institute of Chemical Physics and Biophysics, Akadeemia Tee 23, Tallinn, Estonia

Received February 4, 2004; revised March 23, 2004

## Abstract

$^{17}\text{O}$  NMR studies of various cation-exchanged LTA and LSX zeolites have shown similarities between the two systems. LSX samples containing divalent cations contain resonances with similar chemical shifts to those previously assigned to 'bare' framework oxygen atoms in Ca-LTA and Sr-LTA. The assignments are consistent with the trends seen in the spectra of monovalent cation-containing LSX and LTA zeolites, which show an increase in the average chemical shift with increasing cationic radius. The spectrum of Li-LSX, like Na-LSX, can be assigned based on the T–O–T bond angles. Gas sorption studies on Li-LSX are used to help identify the framework oxygen atoms that form the  $\beta$ -cages and demonstrate the sensitivity of the  $^{17}\text{O}$  shifts to gas loading.  
© 2004 Elsevier Inc. All rights reserved.

## 1. Introduction

Zeolites are a family of microporous aluminosilicates with channels and cavities of molecular dimensions. This structural property has led to many industrial applications of zeolites, which include their use as ion-exchange materials and heterogeneous catalysts [1]. Of the many zeolite topologies known, the synthetic faujasites are the most widely used zeolites for catalytic processes.

An understanding of the interactions that take place between the absorbed species and the zeolite framework is required in order to help develop new catalysts or to improve existing ones. A determination of where different absorbed species bind in the pores of the zeolite and the strength of binding to the different binding sites can also aid in the interpretation of adsorption isotherm data and in the development of materials for gas separations. Magic angle spinning nuclear magnetic resonance (MAS NMR) techniques are excellent for this purpose.  $^{29}\text{Si}$  and  $^{27}\text{Al}$  MAS NMR studies are routinely carried out on zeolites and have contributed significantly to the understanding of the

structural properties of these materials [2,3]. The zeolite framework also contains oxygen and it is through oxygen that the absorbed species often bind to the framework. Therefore the NMR active nucleus of oxygen,  $^{17}\text{O}$ , would be an excellent nucleus with which to study gas binding. However, to date there have been few  $^{17}\text{O}$  NMR studies carried out on zeolites. There are two main reasons for this. Firstly, the natural abundance of  $^{17}\text{O}$  is only 0.037% and secondly it is a  $I = \frac{5}{2}$  quadrupolar nucleus, and the central transitions in  $^{17}\text{O}$  spectra are often broadened noticeably by the second-order quadrupolar interaction. Although the financial cost is high, it is possible to enrich the zeolite with  $^{17}\text{O}$  using either  $^{17}\text{O}$  containing oxygen gas or water [4,5]. Greater resolution can be achieved by using higher magnetic field strengths along with double-angle rotation (DOR) [6], multiple quantum (MQMAS) [7], dynamic-angle spinning (DAS) [8] and satellite transition MAS (STMAS) [9] techniques. Only MQMAS and DOR are used in the work reported in this paper. DOR averages the second-order quadrupole interaction by rotating the sample simultaneously around two angles. This is achieved by placing the sample in a small rotor (known as the inner rotor), which spins inside another rotor (known as the outer rotor). The inner rotor rotates

\*Corresponding author. Fax: +1-631-632-5731.

E-mail address: [cgrey@sbchem.sunysb.edu](mailto:cgrey@sbchem.sunysb.edu) (C.P. Grey).

about an axis inclined at  $30.55^\circ$  to the axis of rotation of the outer rotor, which is spun at the magic angle. MQMAS was introduced by Frydman and Harwood in 1995 [7] and produces a two-dimensional spectrum with an ‘isotropic dimension’ which is free of the broadening caused by the second-order quadrupolar interaction and an ‘anisotropic dimension’ which contains the second-order quadrupolar broadened lineshapes.

Before studies can be carried out on catalytically active materials, information needs to be gathered concerning the factors that affect the  $^{17}\text{O}$  chemical shift. This can be achieved in the first instance by studying different cation-exchanged forms of zeolites at different hydration levels and constructing a database of  $^{17}\text{O}$  chemical shifts. Previous work carried out on  $^{17}\text{O}$  NMR of zeolites includes work on purely siliceous zeolites [5,10] and on Al-substituted zeolites. MQMAS has been used to distinguish between Si–O–Al and Si–O–Si linkages in zeolites such as ZSM-5 [11]. Pingel et al. [12] have reported that the  $^{17}\text{O}$  isotropic shift decreases with increasing Si–O–Al bond angle for hydrated Na-LTA and Na-LSX. Freude and co-workers [13] and Stebbins and co-workers [14] have both studied various cation-exchanged LTA and LSX zeolites species and concluded that the nature of the extra-framework cation and the hydration level have an effect on the chemical shift values. Finally, work by Readman et al. [4] on Ca-A zeolites has shown that the changes in oxygen bonding due to the absence of a nearby extra-framework cation also needs to be considered.

Zeolites LSX and LTA (Fig. 1) were chosen for study as both have a Si:Al ratio of 1:1, therefore in accordance with Löwenstein’s rule [15], only Si–O–Al linkages are present. Zeolites with higher Si:Al ratios will contain a mixture of Si–O–Al and Si–O–Si linkages, complicating the assignment of the spectra. Both LSX and LTA contain  $\beta$ -cages (also known as sodalite cages). In LSX the  $\beta$ -cages are linked by double six-rings (D6R; also known as hexagonal prisms) with large supercages with a pore size of approximately  $13 \text{ \AA}$  formed by the voids between the  $\beta$ -cages. In LTA the  $\beta$ -cages are linked by double four-rings (D4R) and larger  $\alpha$ -cages with an effective pore size of approximately  $5 \text{ \AA}$  are formed by the voids between the  $\beta$ -cages. Crystallographically, there are four distinct oxygen sites in LSX each with a ratio of 1:1:1:1, whereas in LTA there are three crystallographic oxygen atoms with a ratio of 1:1:2.

## 2. Experimental

The cation exchanged form of LTA were produced from as synthesised LTA (Na-A, Aldrich) using conventional aqueous ion-exchange methods. A solution of the zeolite and the metal nitrate was stirred for approximately 12 h, filtered, washed and the process was

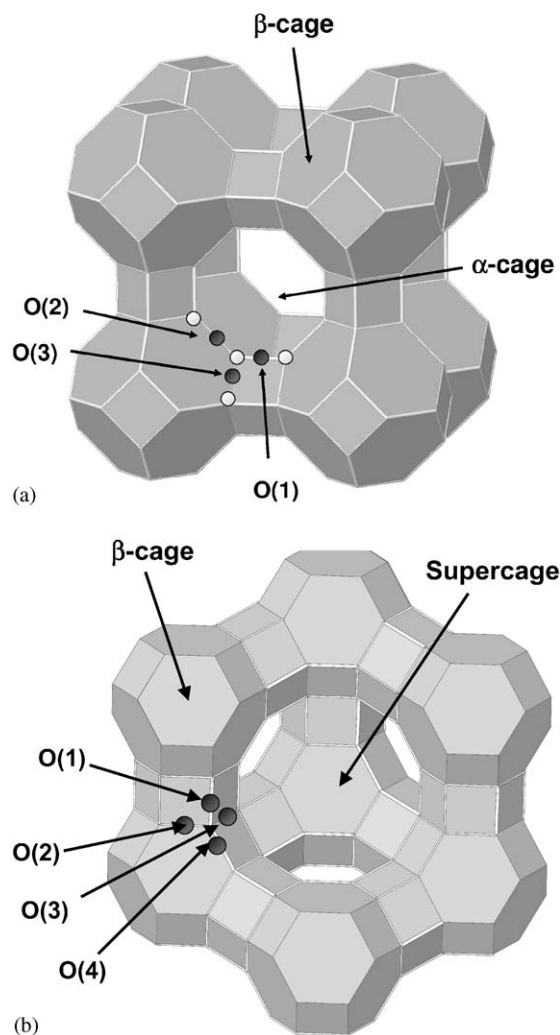


Fig. 1. Schematic representations of (a) zeolite LTA and (b) zeolite LSX. Dark grey atoms represent oxygen atoms, while white represents silicon and aluminium in LTA. For clarity the silicon and aluminium atoms are not shown for LSX. The labelling of the oxygen atoms is consistent with the convention used in published structural studies.

repeated.  $^{23}\text{Na}$  MAS NMR was used to determine the amount of residual sodium in the samples. LSX samples were obtained by ion exchange starting from a solid of composition  $\text{Na}_{77}\text{K}_{19}\text{Si}_{96}\text{Al}_{96}\text{O}_{384}$ . Ion exchange was performed three times for each sample using the appropriate chloride solution. The pH of these solutions were adjusted to pH 8 to maintain crystallinity of the product.  $^{17}\text{O}$  isotopic enrichment was achieved by exposing the dehydrated zeolite ( $500^\circ\text{C}$  for 16 h under vacuum  $> 10^{-3}$  Torr) to  $^{17}\text{O}_2$  gas (40%  $^{17}\text{O}$ , Isotec) at approximately atmospheric pressure and the resulting closed system was heated to  $580^\circ\text{C}$  for 16 h. Exchange levels of not more than 4–6% were achieved, based on spin-counting experiments performed on related systems. Re-hydration of the samples was achieved by suspending the sample above a saturated NaCl solution for several days. The gases were loaded by leaving the

samples exposed to the particular gas in a glove bag. The samples were then packed in DOR rotors and run immediately, since the DOR rotors were not air tight over a long period of time.

$^{17}\text{O}$  MAS NMR experiments were performed on a Bruker DMX 600 MHz (14 T) spectrometer equipped with a 4 mm probe, operating at a frequency of 81.36 MHz for  $^{17}\text{O}$ . For the  $^{17}\text{O}$  1-pulse experiments, a  $\pi/6$  pulse of 1.4 s was used with a recycle delay of 0.5 s and a spinning speed of 13 kHz. Triple quantum MAS experiments were carried out using two high-power pulses of 4.5 and 2.0  $\mu\text{s}$  (rf field strength of 60 kHz), followed by a weak z-filter pulse of 32  $\mu\text{s}$  [16], also at a spinning speed of 13 kHz. For the samples with the greatest enrichment levels 2400 scans were collected per 1D segment of the MQ experiment. For samples where the enrichment level was poorer this was increased to 9600. The length of the MQ experiments varied between 12 and 48 h. All experiments were referenced to  $\text{H}_2\text{O}$ . After 2D processing all spectra were sheared (so as to show the anisotropic and isotropic dimensions along the  $x$ - and  $y$ -axis, respectively) using the shearing function available in the Bruker XWIN-NMR software.

DOR experiments used a home-built probe (NICPB, Tallinn), capable of a 1800 Hz outer rotor rate, although a frequency of 1400 Hz was generally used. The DOR experiments were performed at either 14 (bare samples) or 16.8 T ( $^1\text{H}$  frequency of 720 MHz; gas-loaded samples). Spinning was activated and monitored by a PC operated four-way gas pressure controller. All spectra were acquired with rotor synchronization, effectively doubling the outer spinning rate [17]

### 3. Results and discussion

The  $^{17}\text{O}$  DOR spectra of dehydrated Ca-LSX and Sr-LSX are the  $^{17}\text{O}$  MQMAS spectra of dehydrated Ca-LTA and Sr-LTA are shown in Figs. 2 and 3, respectively. There are clearly similarities between the two sets of spectra. Two sets of resonances are present; one at approximately 70 ppm and another at approximately 30 ppm. Work carried out on Na-LSX and Na-A using both  $^{17}\text{O}$  DOR and MQMAS showed resonances present in the region 30–50 ppm [12]. No resonances were present at the higher frequency range observed here, but a resonance due to the O(3) site has been observed at 75.5 ppm in TI-A [13]. Previous studies on hydrated and dehydrated Ca-A have assigned the peak at approximately 70 ppm in Fig. 3 to the O(1) atoms located in the eight-ring of the  $\alpha$ -cage and that in dehydrated Ca-A have no  $\text{Ca}^{2+}$  cations bound to them (Table 1), i.e., they can be thought of as ‘bare’ oxygen atoms, hydrogen-bonded to the water molecules in the pores of the hydrated zeolites [4]. The assignments of the remaining sites (O(3) and O(2)) are in agreement

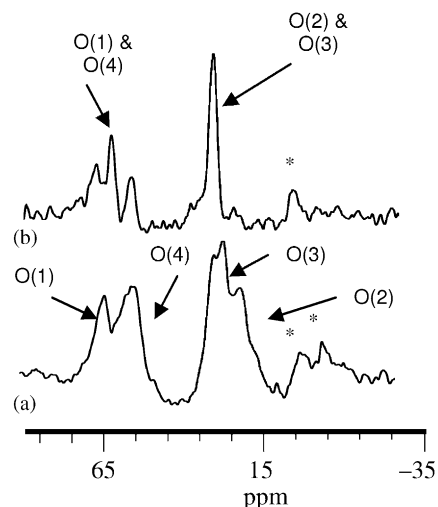


Fig. 2.  $^{17}\text{O}$  DOR spectra of (a) Ca-LSX and (b) Sr-LSX acquired at 14 T. Tentative assignments are as indicated and spinning sidebands are denoted by an asterisk.

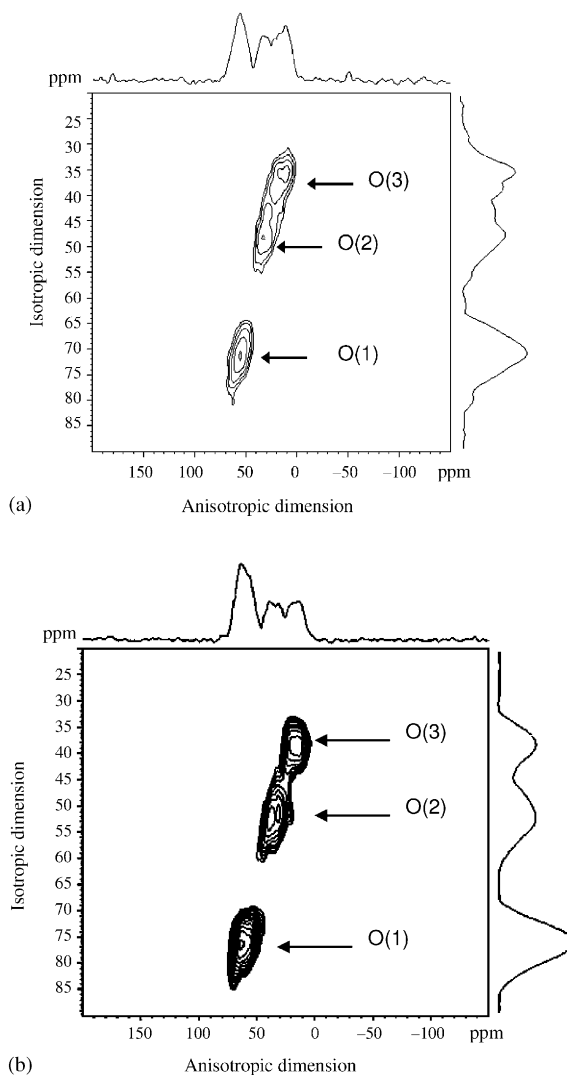


Fig. 3.  $^{17}\text{O}$  MQMAS spectra of (a) Ca-LTA and (b) Sr-LTA. Tentative assignments are as indicated.

Table 1  
Shortest Ca–O distances in Ca-A and Ca-LSX

Ca-A		Ca-LSX	
Ca <sup>2+</sup> –O	Distance (Å)	Ca <sup>2+</sup> –O	Distance (Å)
Ca(1)–O(1)	4.390	Ca(I)–O(1)	3.845
Ca(2)–O(1)	4.664	Ca(I')–O(1)	4.782
Ca(1)–O(2)	2.893	Ca(II)–O(1)	4.400
Ca(2)–O(2)	2.974	Ca(I)–O(2)	3.583
Ca(1)–O(3)	2.270	Ca(I')–O(2)	3.119
Ca(2)–O(3)	2.316	Ca(II)–O(2)	2.274
		Ca(I)–O(3)	2.482
		Ca(I')–O(3)	2.544
		Ca(II)–O(3)	4.274
		Ca(I)–O(4)	5.087
		Ca(I')–O(4)	4.123
		Ca(II)–O(4)	2.778

with the bond-angle, shift correlation of Pingel et al. that states that the larger the T–O–T bond angle, the smaller isotropic chemical shift [12], since T–O–T bond angles of 143°, 165°, 141° for O(1), O(2), and O(3), respectively, have been obtained for hydrated Ca-A [18]. Large shifts were seen for the resonances (in particular the O(1) and O(2) resonances) on dehydration of Ca-A, which was ascribed to the loss of the coordinated water molecules. The assignments for Sr-A made by analogy with the spectrum of Ca-A are consistent with those of Stebbins et al. [13]. Therefore, it is possible that the peaks located at 70 ppm in Ca- and Sr-LSX are also due to ‘bare’ framework oxygen atoms.

Structural studies carried out on dehydrated Ca-LSX by Vitale et al. [19] found three calcium sites. These were located at the site I (at the centre of the hexagonal prism), site I' (displaced from site I into the  $\beta$ -cage) and site II (located in the six-ring of the  $\beta$ -cage). No calcium sites were found in the site II' or site III positions. The main consequence of this cation distribution is that there are no calcium ions within bonding distance to O(1) and O(4) (Table 1). Therefore, we can assign the two peaks at approximately 70 ppm to O(1) and O(4) and those between 30 and 40 ppm as O(2) and O(3). It then appears reasonable to assign the resonances in the two groups using the correlation of Pingel et al. [12]. Hence, given the T–O–T angles resulting from the structural refinement of Vitale et al. [19] (T–O(1)–T 130.4°, T–O(2)–T 141.4°, T–O(3)–T 131.6° and T–O(4)–T 164.3°) we can tentatively assign the peaks from high to low-chemical shift as follows, O(1), O(4), O(3) and O(2). The high-frequency resonances in the Ca-LSX spectrum are presumably better resolved due to the larger separation in bond angles for these oxygen atoms (approximately 34° between O(1) and O(4) and 10° between O(2) and O(3)).

Although, there have been no structural studies carried out on dehydrated Sr-LSX it is known from

structural studies of dehydrated Ca-LTA and Sr-LTA that the Ca<sup>2+</sup> and Sr<sup>2+</sup> cations are located in the same sites in this zeolite [20]. Therefore, it is highly probable that the Sr<sup>2+</sup> cations in Sr-LSX are located in the same sites as Ca-LSX, i.e., the O(1) and O(4) atoms have no Sr<sup>2+</sup> cations coordinated to them and can be considered as being ‘bare’. Therefore, we can assign the peaks at higher chemical shift to the ‘bare’ O(1) and O(4) sites, while those at lower chemical shift to oxygen atoms coordinated to Sr<sup>2+</sup> cations. The overlap between the isotropic resonances and the sidebands in the spectra of both Ca-LSX and Sr-LSX makes any further analysis of the low-frequency resonances difficult with the available data.

<sup>17</sup>O DOR spectra of Na-LSX, K-LSX and Cs-LSX are shown in Fig. 4. <sup>17</sup>O MQMAS spectra of Na-LTA and K-LTA are shown in Fig. 5. A <sup>17</sup>O MQMAS spectrum of Cs-LTA could not be obtained as an <sup>17</sup>O enrichment level high enough to produce good signal to noise could not be achieved. The most probable reason for this is that the large Cs<sup>+</sup> cation blocks the pore openings to the extent that the oxygen gas cannot readily enter. Examination of the spectra shows that there is a shift of the average chemical shift to higher frequency with increasing cation radius. This trend has been observed previously for Na, Sr, K and Tl-A and Na–Cs LSX zeolites [13,14]. This can be rationalised by using the same approach used to assign the spectra of the calcium and strontium analogues. Here, there are no completely ‘bare’ sites as all the cation sites will be either fully or completely occupied and all the

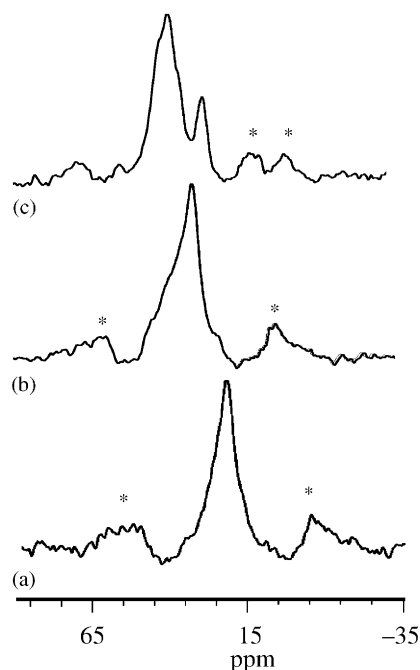
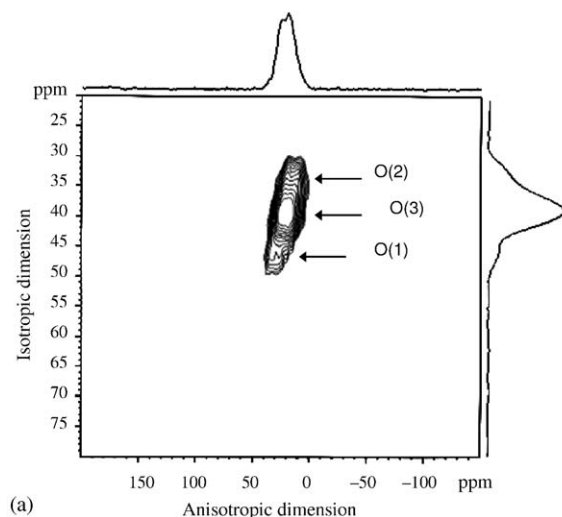
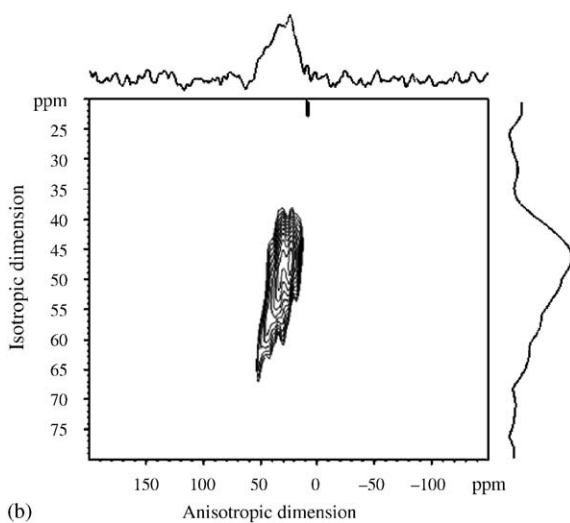


Fig. 4. <sup>17</sup>O DOR spectra of (a) Na-LSX, (b) K-LSX and (c) Cs-LSX acquired at 14 T. Spinning sidebands are denoted by an asterisk.



(a)



(b)

Fig. 5.  $^{17}\text{O}$  MQMAS spectra of (a) Na-LTA and (b) K-LTA. Tentative assignments are as indicated for NaA.

framework oxygen atoms will have a cation bound to them. An increase in the cation radius will result in a larger cation-framework oxygen bond distance, from a Na–O, 2.3 Å [21] to Cs–O, 3.1 Å [22]. The further the cation is away from the framework oxygen atom, the more ‘bare’ that oxygen atom becomes. Weaker (or no) cation–O interactions will result in more basic oxygen atoms, which, as suggested earlier by Freude et al. [13] will result in a larger paramagnetic contribution to the  $^{17}\text{O}$  shift, the shifts seen in Ca and Sr zeolites representing the extreme situation. Some of the LSX spectra show poor resolution and many of the individual peaks cannot be distinguished. This can be rationalised by examining the T–O–T bond angles from structural studies on Na-LSX and K-LSX [23]. For Na-LSX the bond angles are 134.2°, 140.6°, 137.1° and 145.2° for O(1) to O(4), respectively. For K-LSX the angles are 133.1°, 148.8°, 143.5° and 145.5° for O(1) to O(4), respectively. The oxygen bond angles are sufficiently

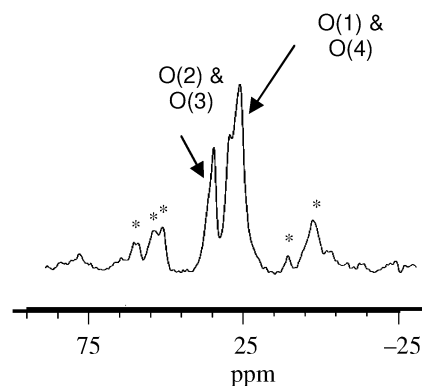


Fig. 6.  $^{17}\text{O}$  DOR spectrum of Li-LSX. Tentative assignments are as indicated and spinning sidebands are denoted by an asterisk.

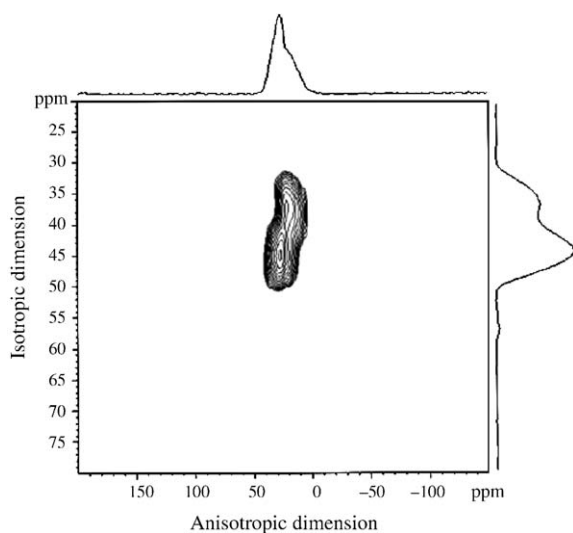


Fig. 7.  $^{17}\text{O}$  MQMAS spectrum of Li-LTA.

close to produce a significant amount of overlap in our  $^{17}\text{O}$  DOR spectra. Four sites were, however, observed in the DOR and 5QMAS spectra of a sample of LSX containing both Na and K ions [13], suggesting that small changes in the extent of ion-exchange can influence these spectra noticeably.

The  $^{17}\text{O}$  DOR spectrum of Li-LSX and MQMAS spectrum of Li-LTA are shown in Figs. 6 and 7, respectively. It can be seen that there are again two regions in the Li-LSX spectrum, one at approximately 37 ppm and the second at approximately 25 ppm. For Li-LTA two broad resonances are observed with similar chemical shifts. There are no known structural studies carried out on Li-LTA produced under the same ion-exchange conditions as presented here. Structural studies carried out on Li-LSX show that  $\text{Li}^+$  cations occupy all possible sites and are nearby all 4 oxygen atoms. The short Li–O bond lengths of 1.88–2.01 Å present in this material [22], are consistent with the small chemical shifts for all the resonances. Based on the bond angle theory of Pingel et al. [12], since the T–O–T bond angles are 143.8°,

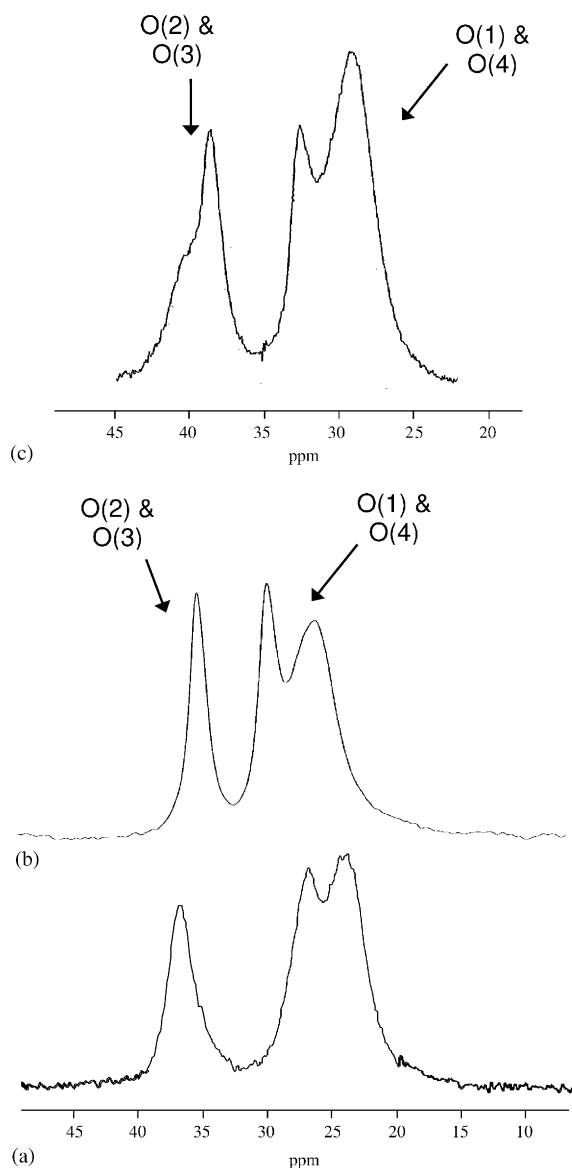


Fig. 8.  $^{17}\text{O}$  DOR spectra of Li-LSX loaded with (a) molecular nitrogen and (b) molecular oxygen acquired at 16.8 T. Tentative assignments are as indicated and spinning sidebands are denoted by an asterisk. The  $^{17}\text{O}$  DOR spectra acquired at 14 T in air is provided in (c) for comparison.

128.6°, 125.6° and 138.6° for O(1) to O(4), respectively [22], we assign the resonances at 25 ppm to O(1) and O(4) and those at 37 ppm to O(2) and O(3).

In order to confirm these assignments  $^{17}\text{O}$  DOR studies were carried out on Li-LSX loaded with nitrogen and oxygen (Fig. 8). Previous studies involving the loading of gases into zeolites have shown that with LSX, nitrogen and oxygen will only fit into the supercage as they are too large to fit into the  $\beta$ -cage [24]. Therefore, we would expect the oxygen atoms accessible from the supercage to be more strongly effected by loading with these gases (i.e., O(1) and O(4)). A change in

the chemical shift of the peaks assigned as O(1) and O(4) from 25 to 30 ppm is observed upon loading with oxygen, while those assigned as O(2) and O(3) shift only slightly to lower frequencies. A shift from lower to higher frequency upon oxygen loading was observed in the  $^7\text{Li}$  MAS NMR studies of Li-LSX carried out by Feuerstein and Lobo [25], where the shift to higher frequency was ascribed to the paramagnetism of the oxygen molecules. Thus, the shifts seen in the  $\text{O}_2$ -absorbed spectrum are consistent with our assignments.

The work presented here, and in earlier papers [13,14] suggests an inverse correlation between the strength of cation-oxygen binding, and the size of the  $^{17}\text{O}$  chemical shift. This result does not agree with the  $^{17}\text{O}$  chemical shifts obtained from first principles calculations of  $\text{Ca}^{2+}$  bound to small aluminosilicate clusters [26]. Here, a shift of approximately 10 ppm to higher frequencies was seen for the Si–O–Al bridging oxygen on  $\text{Ca}^{2+}$  binding, when comparing clusters with similar Si–O–Al bond angles. The results were obtained on very small clusters (with different charges) and it is clear that more detailed calculations are required to develop systematic trends and to help rationalise the effect of the extraframework cations on the shifts.

#### 4. Conclusions

The work presented here shows that there are similarities in the  $^{17}\text{O}$  NMR spectra of two different zeolites that contain the same  $\beta$ -cages, namely LSX and LTA. The samples that have been ion-exchanged with divalent cations show peaks at higher frequencies than those containing only monovalent cations. Examination of structural data appears to suggest that the set of resonances with larger chemical shifts are due to framework oxygen atoms with no cations coordinated to them. The two resonances at higher frequencies and the two resonances at lower frequencies (due to O coordinated to  $\text{Ca}^{2+}$ ) in Ca-LSX can then be assigned using the bond angle correlation of Pingel et al. [12].

For the LSX samples containing the monovalent cations  $\text{Na}^+$ ,  $\text{K}^+$  and  $\text{Cs}^+$ , individual peaks cannot be resolved in this study. Examination of structural data indicates that the Si–O–Al bond angles are similar enough to produce similar chemical shift values. However, a trend of increasing chemical shift with increasing cation radius was observed. For Li-LSX the Si–O–Al bonds angles are sufficiently different for individual peaks to be resolved. As every framework oxygen atom is coordinated to a lithium cation the correlation between T–O–T bond angle and chemical shift could be used to assign the spectrum. Studies of Li-LSX loaded with  $\text{O}_2$  and  $\text{N}_2$  show that the chemical shifts of the resonances are sensitive to gas binding, even for these weakly bound gases.

This work has shown that chemical shift assignments of the crystallographically more simple zeolite LTA can be applied to help assign spectra of the larger pore zeolite LSX. This knowledge will be valuable when studying increasingly more complex zeolites and other gas-loaded samples.

### Acknowledgments

We dedicate this paper to Ray Dupree in recognition of his major role in instigating this work. Ray's incredible knowledge of silicates and solid state NMR was invaluable to this project. Financial support from the Basic Energy Sciences program of the Department of Energy is gratefully acknowledged (DEF-G0296ER14681). LB was supported by the CNRS and the Région Pays de Loire. AS is supported by a NATO linkage Grant 1 1312 0154 and would like to acknowledge the Estonian Science Foundation. Use of the NMR facilities at the Warwick, U.K., NHMFL, Florida, Technical University, Munich, and the Frankfurt University Center for Biomolecular NMR, is greatly appreciated. We are also grateful to the Deutsche Forschungsgemeinschaft project Mi 390/5-2 and to Professor Dr. D. Michel, University of Leipzig, Germany for providing 750 MHz solid-state NMR time.

### References

- [1] D.W. Breck, *Zeolite Molecular Sieves: Structure, Chemistry and Use*, Wiley, New York, 1974.
- [2] J. Klinowski, *Prog. NMR Spectrosc.* 16 (1984) 237.
- [3] J. Klinowski, *Anal. Chim. Acta.* 283 (1993) 929.
- [4] J.E. Readman, N. Kim, M. Ziliox, C.P. Grey, *J. Chem. Soc. Chem. Commun.* (2002) 2808.
- [5] L.M. Bull, A.K. Cheetham, T. Anupold, A. Reinhold, A. Samoson, J. Sauer, B. Bussemer, Y. Lee, S. Gann, J. Shore, A. Pines, R. Dupree, *J. Am. Chem. Soc.* 120 (1998) 3510.
- [6] A. Samoson, E. Lippmaa, A. Pines, *Mol. Phys.* 65 (1988) 1013.
- [7] L. Frydman, J.S. Harwood, *J. Am. Chem. Soc.* 117 (1995) 5367.
- [8] B.F. Chmelka, K.T. Mueller, A. Pines, J. Stebbins, Y. Wu, J.W. Zwanziger, *Nature* 339 (1989) 42.
- [9] Z.H. Gan, *J. Chem. Phys.* 114 (2001) 24.
- [10] L.M. Bull, B. Bussemer, T. Anupold, A. Reinhold, A. Samoson, J. Sauer, A.K. Cheetham, R. Dupree, *J. Am. Chem. Soc.* 122 (2000) 4948.
- [11] J.-P. Amoureux, F. Bauer, H. Ernst, C. Fernandez, D. Freude, D. Michel, U.-T. Pingel, *Chem. Phys. Lett.* 285 (1998) 10.
- [12] U.-T. Pingel, J.-P. Amoureux, T. Anupold, F. Bauer, H. Ernst, C. Fernandez, D. Freude, A. Samoson, *Chem. Phys. Lett.* 294 (1998) 345.
- [13] D. Freude, T. Loeser, D. Michel, U. Pingel, D. Prochnow, *Solid State Nucl. Magn. Reson.* 20 (2001) 46.
- [14] P.S. Neuhoff, P. Zhao, J.F. Stebbins, *Micropor. Mesopor. Mater.* 55 (2002) 239.
- [15] W. Löwenstein, *Am. Mineral.* 39 (1954) 92.
- [16] J.-P. Amoureux, C. Fernandez, S. Steuernagel, *J. Magn. Reson. Ser. A* 123 (1996) 116.
- [17] A. Samoson, E. Lippmaa, *J. Magn. Reson.* 84 (1989) 410.
- [18] W. Thoni, *Z. Kristallogr.* 142 (1975) 142.
- [19] G. Vitale, L.M. Bull, R.E. Morris, A.K. Cheetham, B.H. Toby, C.G. Coe, J.E. MacDougall, *J. Phys. Chem.* 99 (1995) 16087.
- [20] J.J. Pluth, J.V. Smith, *J. Am. Chem. Soc.* 104 (1982) 6977.
- [21] J.J. Pluth, J.V. Smith, *J. Am. Chem. Soc.* 102 (1980) 4704.
- [22] N.H. Heo, K. Seff, *J. Am. Chem. Soc.* 109 (1987) 7986.
- [23] Y. Lee, S.W. Carr, J.B. Parise, *Chem. Mater.* 10 (1998) 2561.
- [24] J. Plévert, F. Di Renzo, F. Fajula, G. Chiari, *J. Phys. Chem. B* 101 (1997) 10340.
- [25] M. Feuerstein, R. Lobo, *J. Chem. Soc. Chem. Commun.* (1998) 1647.
- [26] X. Xue, M. Kanzaki, *J. Phys. Chem. B* 103 (1999) 10816.